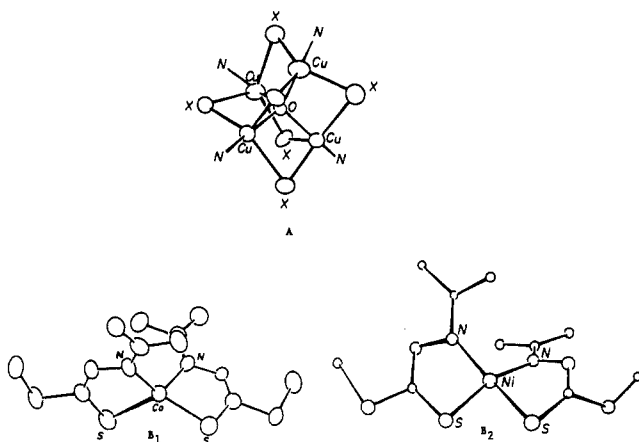




**Table I.** Analytical, Cryoscopic Molecular Weight, and Electronic Spectral Data for Transmetalation Targets and Products

complex	anal., <sup>a</sup> %								$M_r^b$	$\lambda_{\text{max}},^c$ nm ( $\epsilon_\lambda, \text{M}^{-1} \text{cm}^{-1}$ )	
	C	H	N	Cl	Cu	Ni	Zn	Co			
<b>A. Targets</b>											
$\text{N}_4\text{Cu}_4\text{Cl}_6\text{O}^d$	40.0 (40.0)	4.7 (4.7)	9.2 (9.7)	17.7 (17.8)	21.0 (21.2)					$1180 \pm 20$ (1196)	850 (1630), 775 (1400)
$\text{N}_4\text{Cu}(\text{Ni}(\text{H}_2\text{O}))_3\text{Cl}_6\text{O}^d$	36.5 (38.9)	4.7 (5.1)	8.7 (9.1)		5.5 (5.1)	14.1 (14.3)				$1200 \pm 20$ (1236)	850 (360), 775 (340)
$\text{N}_4\text{Cu}(\text{Ni}(\text{H}_2\text{O}))_3\text{Br}_6\text{O}^d$	32.0 (31.9)	4.1 (4.1)	7.6 (7.5)		4.2 (4.2)	11.9 (11.7)				$1500 \pm 20$ (1502)	850 (355), 775 (330)
<b>B. Products</b>											
$\text{N}_4(\text{Ni}(\text{H}_2\text{O}))_3\text{ZnCl}_6\text{O}$	37.6 (38.9)	4.8 (5.0)	8.8 (9.1)	16.7 (17.0)		14.1 (14.3)	5.1 (5.3)			$1250 \pm 20$ (1234)	<i>e</i>
$\text{N}_4(\text{Ni}(\text{H}_2\text{O}))_3\text{ZnBr}_6\text{O}$	30.9 (31.9)	3.8 (4.1)	7.2 (7.4)			11.2 (11.8)	3.9 (4.3)			$1515 \pm 20$ (1504)	850 (80), 775 (83)
$\text{N}_4(\text{Ni}(\text{H}_2\text{O}))_3\text{CoCl}_6\text{O}^f$	37.9 (39.0)	4.7 (5.0)	8.7 (9.1)	16.7 (17.1)		13.8 (14.4)		4.2 (4.8)		$1240 \pm 20$ (1228)	630 (350), 610 (420)
$\text{N}_4(\text{Ni}(\text{H}_2\text{O}))_4\text{Cl}_6\text{O}$	37.8 (38.5)	5.1 (5.2)	8.7 (9.0)			18.5 (18.8)				$1270 \pm 20$ (1249)	<i>e</i>

<sup>a</sup> Calculated values in parentheses. <sup>b</sup> Measured cryoscopically in nitrobenzene at the  $(3\text{--}5) \times 10^{-2}$  m level.<sup>3</sup> <sup>c</sup> In nitrobenzene. <sup>d</sup> Electronic data from ref 9. <sup>e</sup> Negligible molar absorptivities in the region 775–860 nm. <sup>f</sup> Identical data were obtained for the products of eqs 9 (reactant B<sub>1</sub>) and 10 (reactant E).



**Figure 1.** Core molecular structures of A,<sup>2</sup> bis(S-methyl isopropylidenehydrazinecarbodithioato)cobalt(II)<sup>7</sup> (B<sub>1</sub>), and bis(S-methyl isopropylidenehydrazinecarbodithioato)nickel(II)<sup>5</sup> (B<sub>2</sub>). Bis(S-methyl isopropylidenehydrazinecarbodithioato)zinc(II) (B<sub>3</sub>) is isomorphous with B<sub>1</sub>.<sup>7</sup>

transmetalator, that depend on the identities of X, M, and NS.<sup>8,9</sup> From the observation of third- and first-order rate laws 2 and 4 and the known Lewis acid properties of B,<sup>12</sup> we proposed that rate laws 2–4 arise from the involvement of rapidly equilibrated transmetalation precursors (eq 5) whose different stoichiometries (*n*) and stabilities ( $\beta_n$ ) depend on X, M, and NS. From structural information on the reactants<sup>2,5–7</sup> we proposed that these precursors contain four-membered  $\text{Cu-X-M-S}$  rings R formed with an X atom from A and a carbothioate S atom from B or C. It would appear that rings R facilitate metal exchange leading to the efficient transmetalation of A.<sup>8–10</sup>

We recently concluded<sup>10</sup> from activation parameter correlations that rate law 4 is a special case of rate law 3 that involves especially stable 1:1 precursors (i.e., large  $\beta_1$ ). The primary factor leading to rate law 4 is the presence of X = Br in the target.<sup>8–10</sup> However, eqs 2–4 cannot be used to obtain the actual values of  $\beta_n$  and so no direct comparison of precursor stabilities and reaction rates could be made.<sup>8–11</sup>

One important benefit of eq 1 is that each step is stoichiometric.<sup>3,4</sup> Equation 1 can thus be used to generate any particular member of the product family  $(\mu_4\text{-O})\text{N}_4\text{Cu}_{4-x}\text{M}_x\text{X}_6$ <sup>3,4</sup> with fixed X, such as  $(\mu_4\text{-O})\text{N}_4\text{Cu}(\text{Ni}(\text{H}_2\text{O}))_3\text{Cl}_6$  (D),<sup>3,13</sup> which can then

be studied as a target for transmetalation by  $\text{M}(\text{NS})_n$  reagents. Kinetic studies of such individual systems give valuable information on how the rates and rate laws of transmetalation of  $(\mu_4\text{-O})\text{N}_4\text{Cu}_{4-x}\text{M}_x\text{X}_6$  targets change with the occupancy, *x*, of a given core structure by M. Kinetic reproducibility of different samples of isolated<sup>2–4,13</sup> targets such as D would further demonstrate<sup>3,4</sup> that eq 1 is a source of easily separated, pure heteropolymetallic products.

This paper reports that the one remaining copper(II) center in D is specifically replaced by M = Co or Zn from transmetalators B and  $\text{Co}(\text{NS})_3$ , E.<sup>14,15</sup> Although A and D are both monotransmetalated by B (M = Ni (B<sub>2</sub>)) with rate law 2, the reactions of D with B (M = Co (B<sub>1</sub>) and Zn (B<sub>3</sub>)) are governed by new rate law 6, which can be used to determine individual values of

$$\text{rate} = k_4\beta_1[\text{B}][\text{D}]/(1 + \beta_1[\text{D}]) \quad (6)$$

$k_4$  and  $\beta_1$  in eqs 4 and 5, respectively. An important finding of this work is that different forms of 1:1 precursor B<sub>3</sub>D exist at different temperatures and that they are converted to products at different rates. The data also show for the first time that more stable transmetalation precursors are converted to metal-exchanged products at lower rates and that the activation parameters  $\Delta H_4^\ddagger$  and  $\Delta S_4^\ddagger$  for rate laws 4 and 6 are strongly correlated.

## Experimental Section

**Materials and Methods.** Procedures of synthesis and for stoichiometric transmetalation of A and D by B and  $\text{Co}(\text{NS})_3$  (E) and for isolation and characterization of the respective products have been described previously.<sup>2–4,8–11,13</sup> Analytical, cryoscopic, and electronic spectral data for the targets and products of this study are collected in Table I.

**Kinetic Measurements.** All kinetic measurements were conducted in anhydrous nitrobenzene under dinitrogen with a sufficient stoichiometric excess of target D to ensure monotransmetalation under pseudo-first-order conditions, as described previously.<sup>8–11</sup> Initial concentrations of D were varied in the range  $10^4[\text{D}]_0 = 2.5\text{--}25.0$  M with  $[\text{TM}]_0$  fixed at  $2.5 \times 10^{-5}$  M. Temperature was varied from 8.0 to 45.0 °C. Monitoring wavelengths in the thermostated Hi-Tech SFL40 stopped-flow spectrophotometer were in the range 575–650 nm. All reactions were monitored for at least 10 half-lives. On-line computer-generated<sup>11</sup> plots of  $\ln(A_\infty - A_t)$  vs time gave the pseudo-first-order rate constant,  $k_{\text{obsd}}$ , for each set of fixed experimental conditions. Each run was repeated at least five times and each  $k_{\text{obsd}}$  was reproducible to  $\pm 5\%$  or better. Errors in rate and equilibrium constants and their associated thermodynamic parameters were determined by standard least-squares methods.<sup>11</sup> There were

(12) Iskander, M. F.; El-Sayed, L.; Labib, L.; El-Toukhy, A. *Inorg. Chim. Acta* **1984**, *86*, 197.

(13) The nickel centers of isolated<sup>2–4</sup>  $(\mu_4\text{-O})\text{N}_4\text{Cu}_{4-x}\text{Ni}_x\text{X}_6$  each contain one coordinated water molecule.

(14) (a) Davies, G.; El-Sayed, M. A.; El-Toukhy, A.; Henary, M.; Gilbert, T. R. *Inorg. Chem.* **1986**, *25*, 2373. (b) Davies, G.; El-Sayed, M. A.; El-Toukhy, A.; Henary, M.; Kasem, T. S.; Martin, C. A. *Inorg. Chem.* **1986**, *25*, 3904.

(15) Transmetalator E crystallizes as the green *fac* isomer, which rapidly isomerizes to the brown *mer* isomer in aprotic solvents: Onan, K. D.; Davies, G.; El-Sayed, M. A.; El-Toukhy, A. *Inorg. Chim. Acta* **1986**, *119*, 121. The *mer* isomer of E was used throughout this work.

no significant kinetic effects of using different samples of B, D, or E. Raw kinetic data for each system are collected in Table II.<sup>16</sup>

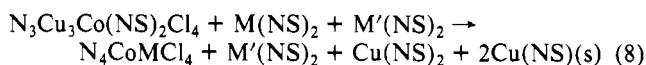
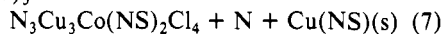
### Results and Discussion

**General Observations.** The heteropolymetallic products of eqs 1 with  $x = 1-4$  are easily isolated from coproduct  $\text{Cu}(\text{NS})_2$  by gel permeation chromatography on Biobeads SX-12 resin with methylene chloride as the eluent.<sup>2-4</sup> However, this method is incapable of separating different members of a  $(\mu_4\text{-O})\text{N}_4\text{Cu}_{4-x}\text{M}_x\text{X}_6$  family from each other. Thus, reactions 1 conducted at fixed  $x$  could conceivably give inseparable mixtures of products  $(\mu_4\text{-O})\text{N}_4\text{Cu}_{4-x}\text{M}_x\text{X}_6$  with varying  $x$ . We therefore carefully checked the analytical and spectral reproducibility of different samples of D obtained with  $x = 3$  in eq 1 at different reactant concentrations. We also checked the kinetic reproducibility of these samples as targets for transmetalation with each transmetalator of this study. The results showed that eq 1 generates D that is not contaminated with coproduct  $\text{Cu}(\text{NS})_2$  or with products with different  $x$  after gel permeation chromatographic separation.

Our previous work shows that the monotransmetalation of polynuclear halocopper(I)<sup>11</sup> and copper(II)<sup>8-10</sup> targets by *S*-methyl hydrazinecarbodithioate transmetalators B and C is, with very few exceptions,<sup>11</sup> governed by one or other of eqs 2-4. Equation 3 appears to be characteristic of transmetalators C, whereas rate laws 2-4 have been established for transmetalators B, depending on the particular transmetalation system.<sup>8-10,11</sup> Rate law 4 has never been observed with dimeric copper(I) targets.<sup>10,11</sup>

Equations 2 and 3 were interpreted to indicate the involvement of rapidly formed but thermodynamically weak precursors  $\text{TM}\cdot\text{A}_2$  and  $\text{TM}\cdot\text{A}$ , respectively, in eq 5. Thermodynamic data for other weak B- and C-adduct systems<sup>12</sup> were used to derive activation entropies  $\Delta S^\ddagger$  for first-order, rate-determining conversion of  $\text{TM}\cdot\text{A}_2$  and  $\text{TM}\cdot\text{A}$  to metal-exchanged products for comparison with data associated with rate law 4. The latter arises because particularly strong precursors are formed in certain transmetalation systems.<sup>9,10</sup> In such cases no assumptions have to be made to interpret the rate data because the observed first-order rate constant  $k_{\text{obsd}} = k_4$  directly refers to the rate-determining step. On this basis we tried to decide whether metal exchange in a particular system is faster than formation of the ultimate transmetalation products. We concluded that metal exchange in weak  $\text{Cu-X-M-S}$  rings is fastest when nucleophilic thiocarboate S is derived from the *S*-methyl isopropylidene ligand system of thermodynamically weak<sup>14b</sup> complexes  $\text{B}_1$  and  $\text{B}_3$ .<sup>10</sup>

Other work demonstrates that the demetalation and transmetalation of heteropolynuclear metal complexes derived from copper(I) and copper(II) targets is metal-specific.<sup>14b</sup> For example, when the mixed-valence product of eq 7 is reacted with equimolar  $\text{N}_4\text{Cu}_4\text{Cl}_4 + \text{Co}(\text{NS})_3 \rightarrow$



transmetalators B (eq 8, M and M' are different metals), the dimeric product contains only M, the metal that forms the thermodynamically weaker  $\text{M}(\text{NS})_2$  complex.<sup>14b,17</sup> These observations<sup>14b</sup> indicate that the relative thermodynamic stability of competing transmetalators B or C is important in determining reaction specificity. However, another contributing factor could be that different transmetalators react with a particular target with different rate laws. This would make the relative rates of competing reactions different in particular systems. Kinetic measurements thus might reveal the structural-mechanistic origins of demetalation and transmetalation specificity.

The following questions are addressed in this paper.

(1) Targets A can be progressively transmetalated with reagent  $\text{B}_2$  to give the family of copper(II)-nickel(II) products of eq 1.<sup>3</sup>

Is copper(II) in these products specifically replaced by other metals M?

(2) Do the rates and rate laws for reactions of A and D with particular transmetalators B differ?

(3) Rate laws 2 and 3 indicate the involvement of very weak transmetalation precursors in eq 5, while rate law 4 is consistent with very strong target-transmetalator interactions in particular circumstances. Are there any systems in which moderately strong interactions give rise to new rate law forms from which direct thermodynamic data for precursor formation can be derived?

As we shall see, A and D react with particular transmetalators with sharply different rates and rate laws. The rate and rate law differences are a valuable source of new information on the structural requirements for specific transmetalation.

**Targets A and D.** Target A ( $\text{X} = \text{Cl}$ ) (Figure 1) consists of four copper(II) centers tetrahedrally attached to a central oxo group. Each pair of copper atoms is bridged by Cl, and each metal center carries a monodentate pyridine ligand N in a local trigonal-bipyramidal geometry.<sup>2</sup>

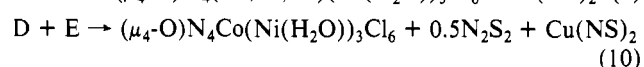
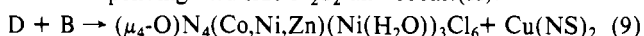
The heteropolymetallic products from eq 1 ( $x = 1-3$ ) are solids, but they cannot be crystallized without disproportionating to A.<sup>3,4</sup> We characterize them by complete elemental analysis and by cryoscopic and spectral measurements. Their analytical, cryoscopic, and spectral properties indicate the same tetranuclear core structure as in A.<sup>3,4</sup> The only major difference is that the nickel centers of isolated  $(\mu_4\text{-O})\text{N}_4\text{Cu}_{4-x}(\text{Ni}(\text{H}_2\text{O}))_x\text{X}_6$  products each have one coordinated water molecule in addition to N. This water is coordinated during gel permeation chromatographic separation and makes each nickel center six-coordinate.<sup>2,3,13</sup>

In principle, either nickel or copper in D could be replaced by another metal M provided the stability order is  $\text{Cu}(\text{NS})_2, \text{Ni}(\text{NS})_2 \gg \text{M}(\text{NS})_2$ . This criterion is satisfied with  $\text{B}_1, \text{B}_3$ , and E.<sup>14b</sup>

**Transmetalators B.** X-ray structural data<sup>7</sup> indicate that  $\text{B}_1$  and  $\text{B}_3$  are both tetrahedral molecules (Figure 1). One side of each molecule is effectively shielded by the isopropylidene groups of B in van der Waals contact. This may affect the ability of the two thiocarboate S atoms on the other side of each molecule to form a transmetalation precursor with one or two molecules of A or D.<sup>7-10</sup>

On the other hand,  $\text{Ni}(\text{NS})_2$  ( $\text{B}_2$ ) (Figure 1) is essentially a flat molecule (the dihedral angle is  $27^\circ$ ) with a *cis*-S geometry.<sup>5</sup> This geometry apparently allows  $\text{B}_2$  to form precursors of stoichiometry  $\text{B}_2\cdot\text{A}_2$  in rate law 2. However, rate law 2 indicates that such precursors are thermodynamically weak.<sup>9,11</sup>

**Monotransmetalation of  $(\mu_4\text{-O})\text{N}_4\text{Cu}(\text{Ni}(\text{H}_2\text{O}))_3\text{Cl}_6$  (D) with B and E. Properties of the Products.** Spectrophotometric titrations at 600 nm, where coproduct  $\text{Cu}(\text{NS})_2$  is the principal absorber,<sup>2,4</sup> indicated that D reacts stoichiometrically with 1 mol of B or E. The analytical and electronic spectral data in Table I show that the monotransmetalation of D with B or E results in exclusive replacement of copper(II) with Co or Zn. The observed reactions are eqs 9 and 10. The first product of eq 10 contains cobalt(II) because of rapid decomposition of primary  $\text{Co}^{\text{III}}(\text{NS})$  centers to the corresponding disulfide  $\text{N}_2\text{S}_2$  and cobalt(II).<sup>4,14</sup>



The products of these monotransmetalation reactions are unassociated tetramers in nitrobenzene (Table I). Their infrared spectra exhibit a single, sharp feature at  $1630 \text{ cm}^{-1}$ , which is diagnostic of the bonding of *N,N*-diethylnicotinamide through its pyridine N atom.<sup>18</sup>

The electronic spectral data in Table I indicate that molar absorptivities of D and its monotransmetalation products at 850 nm increase with atomic copper content and that those at 610 nm increase with atomic cobalt content. Spectral data for a wide range of analytically pure products of transmetalation of  $(\mu_4\text{-O})(\text{N}, \text{py})_4\text{Cu}_4\text{X}_6$  complexes (py is pyridine) with a range of  $\text{M}(\text{NS})_n$

(16) Table II and Figures 5 and 6 are given as supplementary material.

(17) The appearance of dimeric products in eq 8 is due to intramolecular NS ligand transfer from cobalt(II) to copper(II).<sup>14</sup>

(18) Davies, G.; El-Toukhy, A.; Onan, K. D.; Veidis, M. *Inorg. Chim. Acta* **1985**, *98*, 85.



**Table III.** Kinetic Data for First-Order Systems

target	TM	$k^a$	$\Delta H^{*b}$	$\Delta S^{*c}$	ref
A. Kinetic Data for Transmetalation					
$N_4Cu(Ni(H_2O))_3Cl_6O$	$Zn(NS)_2$	27.5	$29.0 \pm 0.4$	$46 \pm 3$	<i>d</i> , LT <sup>e</sup>
$N_4Cu(Ni(H_2O))_3Cl_6O$	$Zn(NS)_2$	8.0	$17.0 \pm 0.3$	$4 \pm 3$	<i>d</i> , HT <sup>f</sup>
$N_4Cu(Ni(H_2O))_3Cl_6O$	$Co(NS)_2$	3.3	$8.5 \pm 0.3$	$-28 \pm 3$	<i>d</i>
$N_4Cu(Ni(H_2O))_3Cl_6O$	$Co(NS)_3$	1.5	$9.5 \pm 0.3$	$-25 \pm 3$	<i>d</i>
$N_4Cu(Ni(H_2O))_3Br_6O$	$Zn(NS)_2$	7.3	$14.7 \pm 0.4$	$-5 \pm 3$	<i>d</i>
$N_4Cu_2(Ni(H_2O))_2Cl_6O$	$Zn(NS)_2$	4.2	$21.1 \pm 0.4$	$16 \pm 3$	24
$py_4Cu_2(Ni(H_2O))_2Cl_6O$	$Zn(NS)_2$	5.0	$21.8 \pm 0.4$	$18 \pm 3$	24
B. Kinetic Data for Complexation					
$N_4Cu(Ni(H_2O))_3Cl_6O$	$Cu(NS)_2$	3.2	$14.0 \pm 0.3$	$-9 \pm 3$	24
$N_4Cu_2(Ni(H_2O))_2Cl_6O$	$Cu(NS)_2$	3.8	$16.0 \pm 0.4$	$1 \pm 2$	24
C. Kinetic Data for Dissociation of T-Cu(NS) <sub>2</sub> Complexes					
$N_4Cu_4Cl_6O-Cu(NS)_2$		0.045	$19.7 \pm 0.4$	$1 \pm 1$	24
$N_4(Ni(H_2O))_4Cl_6O-Cu(NS)_2$		0.056	$19.4 \pm 0.3$	$1 \pm 1$	24

<sup>a</sup>The rate constants and activation parameters in sections A, B, and C of this table refer to transmetalation rate laws 4 and 6, complexation with rate law 4,<sup>24</sup> and complex dissociation ( $k$ , term of rate law 12<sup>11,12</sup>). All rate constant units are  $s^{-1}$  at 23 °C (typical error is  $\pm 5\%$ ). <sup>b</sup>Units are kcal  $mol^{-1}$ . <sup>c</sup>Units are cal  $deg^{-1} mol^{-1}$  at 25 °C. <sup>d</sup>This work. <sup>e</sup>At "low" temperature; see text. <sup>f</sup>At "high" temperature; see text.

we know that changing X from Cl to Br in this target structure tends to favor first-order rate law 4, which indicates especially strong precursors containing terminal Br.<sup>9,10</sup> This reasoning supports the assignment of the data correlated by the third line from the left in Figure 2 to precursors P<sub>2</sub> containing terminal X.

The rate law for reaction of A with  $Ni(NS)_2$  is unaffected by replacement of three of the copper(II) centers in this target with  $Ni(H_2O)$  centers, although the third-order rate constant  $k_2$  increases by a factor of about 200 at 25 °C. This may be partly due to an increase in the stability of the precursor as a result of  $Ni(H_2O)$  substitution for copper in A. The activation parameter data for reaction of D with  $Ni(NS)_2$  correlate quite well with other third-order data (Figure 2). The observed enthalpy and entropy of activation for this system are the lowest observed for transmetalation of the  $(\mu_4-O)_4N_4Cu_{4-x}(Ni(H_2O))_xCl_6$  family by  $Ni(NS)_2$  with rate law 2, possibly indicating that Ni-Cl bonds are weaker than Cu-Cl bonds in  $(\mu_4-O)_4N_4Cu_{4-x}(Ni(H_2O))_xCl_6$  targets and that this causes an increase in precursor stability, as in P<sub>2</sub>.<sup>20</sup> However, it would appear from the activation parameter correlation in Figure 2 that there is no extensive Ni-Cl bond breaking in this family of reactions that would lead to second- or first-order rate laws 3 or 4, respectively.

From these results it can be assumed that the rate law for transmetalation of the whole  $(\mu_4-O)_4N_4Cu_{4-x}(Ni(H_2O))_xCl_6$  family by  $Ni(NS)_2$  is third-order. We would expect the data to fit the rightmost line in Figure 2, with the rate constants increasing with increasing  $x$ .

Previous work<sup>2-4,8,9</sup> shows that pure products result from the stepwise reactions 1. This implies that the rates of progressive replacement of copper with M either are similar or actually decrease with the extent of transmetalation under anhydrous conditions. The present data do not bear on this question because one water molecule is coordinated to each nickel center during product isolation<sup>3,8,9,13</sup> and the nickel in  $(\mu_4-O)_4N_4Cu_{4-x}(Ni(H_2O))_xCl_6$  is thus six-coordinate. As discussed above, this situation leads to higher rates of replacement of the remaining copper by nickel from  $Ni(NS)_2$ . By contrast, progressive transmetalation in eq 1 is conducted<sup>2-4</sup> under anhydrous conditions so that each new metal center introduced is five-coordinate.

**Rate Law 4.** The monotransmetalation of D by excellent transmetalator E<sup>14</sup> was found to be governed by first-order rate law 4 (Table II).<sup>16</sup> Kinetic data are collected in Table III.

**Differences in Rate Law for the Monotransmetalation of A and D by B<sub>1</sub> and B<sub>3</sub>.** Tetranuclear copper(II) target A is monotransmetalated by B<sub>1</sub> and B<sub>3</sub> with third-order rate law 2.<sup>9</sup> In sharp contrast, we report here that the corresponding reactions of copper-nickel target D are governed by new rate law 6.

**Rate Law 6.** Kinetic and equilibrium data for systems governed by rate law 6 are collected in Tables II,<sup>16</sup> III, and IV. Figures 3 and 4 illustrate rate law 6 for two different transmetalation systems. Rate law 6 can be rearranged to give eq 11. Figures

**Table IV.** Equilibrium Data for Rate Laws 6 and 12 in Nitrobenzene

target	reactant	$\beta_1$ , $K_1^a$	$\Delta H_1^b$	$\Delta S_1^c$	ref
A. Transmetalation Systems					
$N_4Cu(Ni(H_2O))_3Cl_6O$	B <sub>3</sub>	250	$-31.4 \pm 0.4$	$-94 \pm 4$	<i>d</i> , LT <sup>e</sup>
$N_4Cu(Ni(H_2O))_3Cl_6O$	B <sub>3</sub>	1400	$0.8 \pm 0.3$	$17 \pm 4$	<i>d</i> , HT <sup>f</sup>
$N_4Cu(Ni(H_2O))_3Cl_6O$	B <sub>1</sub>	3300	$-2.2 \pm 0.5$	$9 \pm 4$	<i>d</i>
B. Complexation Systems					
$N_4Cu_4Cl_6O$	$Cu(NS)_2^g$	1780	$-20.0 \pm 0.4$	$-53 \pm 3$	24
$N_4(Ni(H_2O))_4Cl_6O$	$Cu(NS)_2^g$	1260	$-6.4 \pm 0.2$	$-8 \pm 2$	24
$(TEED)_2Cu_2Cl_2^h$	$Co(NS)_2^g$	400	$-2.7 \pm 0.3$	$3 \pm 2$	11
$(TEED)_2Cu_2Cl_2$	$Cu(NS)_2^i$	350	$-0.6 \pm 0.2$	$10 \pm 2$	11
$(TEED)_2Cu_2Br_2$	$Cu(NS)_2^i$	560	$8.8 \pm 0.3$	$41 \pm 2$	11

<sup>a</sup>Units are  $M^{-1}$  at 23 °C (typical error is  $\pm 5\%$ ). <sup>b</sup>Units are kcal  $mol^{-1}$ . <sup>c</sup>Units are cal  $deg^{-1} mol^{-1}$  at 25 °C. <sup>d</sup>This work. <sup>e</sup>At "low" temperature; see text. <sup>f</sup>At "high" temperature; see text. <sup>g</sup>NS = S-methyl isopropylidenehydrazinocarbothioate.<sup>11</sup> <sup>h</sup>TEED = *N,N,N',N'*-tetraethyl-ethylenediamine. <sup>i</sup>NS = S-methyl benzylidenehydrazinocarbothioate.<sup>11</sup>

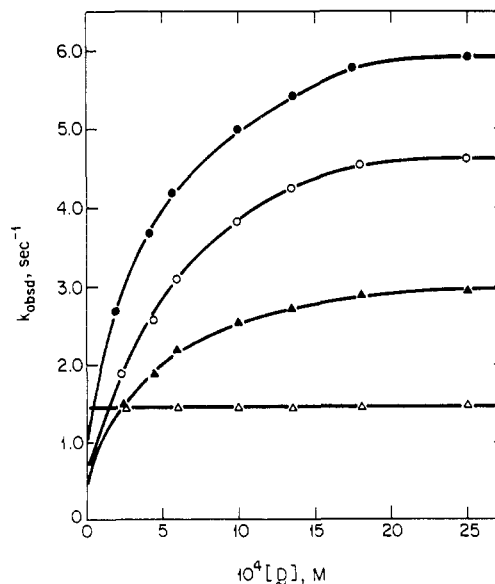


**Figure 3.** Plots of  $k_{obsd}$  ( $s^{-1}$ ) vs  $[D]$  (M) for the monotransmetalation of excess  $(\mu_4-O)_4N_4Cu_{4-x}(Ni(H_2O))_xCl_6$  (D) with  $Co(NS)_2$  (B<sub>1</sub>) in nitrobenzene at the following temperatures: 8.0 °C ( $\Delta$ ); 23.0 °C ( $\blacktriangle$ ); 30.0 °C ( $\circ$ ); 38.5 °C ( $\bullet$ ).

5<sup>16</sup> and 6<sup>16</sup> contain plots of eq 11 for the data in Figures 3 and 4, respectively.

$$1/k_{obsd} = 1/\beta_1 k_4 [D] + 1/k_4 \quad (11)$$

Rate law 6 has never been observed before in a transmetalation system. This rate law form is very useful in interpreting the

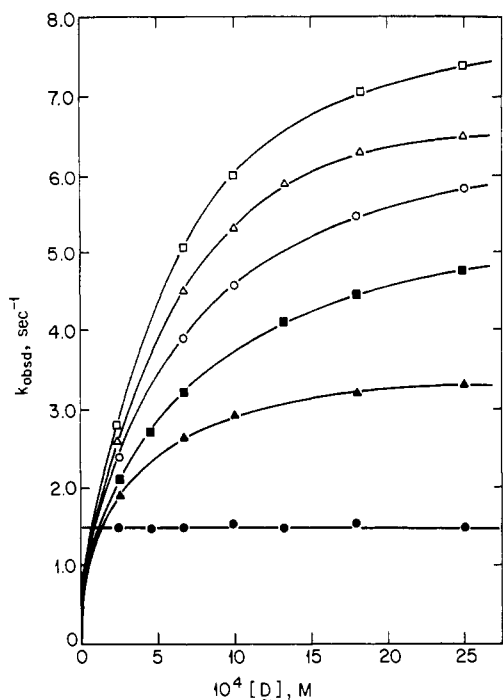


**Figure 4.** Plots of  $k_{\text{obsd}}$  ( $\text{s}^{-1}$ ) vs  $[\text{D}]$  (M) for the monotransmetalation of excess  $(\mu_4\text{-O})\text{N}_4\text{Cu}(\text{Ni}(\text{H}_2\text{O}))_3\text{Cl}_6$  (D) with  $\text{Zn}(\text{NS})_2$  ( $\text{B}_3$ ) in nitrobenzene at the following temperatures: 8.0 °C (●); 10.0 °C (▲); 12.0 °C (■); 15.0 °C (○); 17.5 °C (△); 18.5 °C (□).

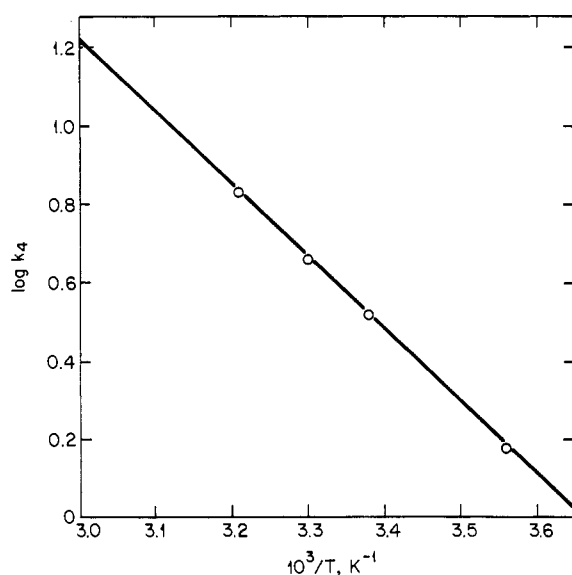


**Figure 7.** Plot of  $\log k_4$  vs  $1/T$  ( $\text{K}^{-1}$ ) for the monotransmetalation of excess  $(\mu_4\text{-O})\text{N}_4\text{Cu}(\text{Ni}(\text{H}_2\text{O}))_3\text{Cl}_6$  (D) with  $\text{Co}(\text{NS})_2$  ( $\text{B}_1$ ) in nitrobenzene.

mechanisms of metal substitution and redox systems<sup>21,22</sup> and is invaluable in understanding specific enzyme-substrate reactions.<sup>23</sup> Its discovery is a very important addition to what is already known about transmetalation rate laws and mechanisms for the following reasons. First, we can determine values of  $\beta_1$  and their associated enthalpies and entropies and compare them with  $K_1$  derived from eq 12 for complex formation reactions with particular targets

$$k_{\text{obsd}} = k_f[\text{target}][\text{Cu}(\text{NS})_2] + k_r \quad (12)$$

$\text{L}_2\text{Cu}_2\text{X}_2$  and  $(\mu_4\text{-O})\text{N}_4\text{Cu}_{4-x}(\text{Ni}(\text{H}_2\text{O}))_x\text{Cl}_6$ <sup>11,24</sup> ( $K_1 = k_f/k_r$ ; the

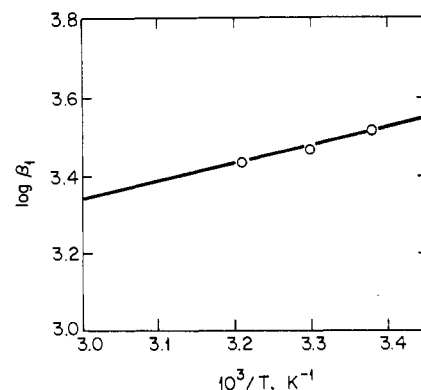


**Figure 8.** Plot of  $\log \beta_1$  vs  $1/T$  ( $\text{K}^{-1}$ ) for the monotransmetalation of excess  $(\mu_4\text{-O})\text{N}_4\text{Cu}(\text{Ni}(\text{H}_2\text{O}))_3\text{Cl}_6$  (D) with  $\text{Co}(\text{NS})_2$  ( $\text{B}_1$ ) in nitrobenzene.

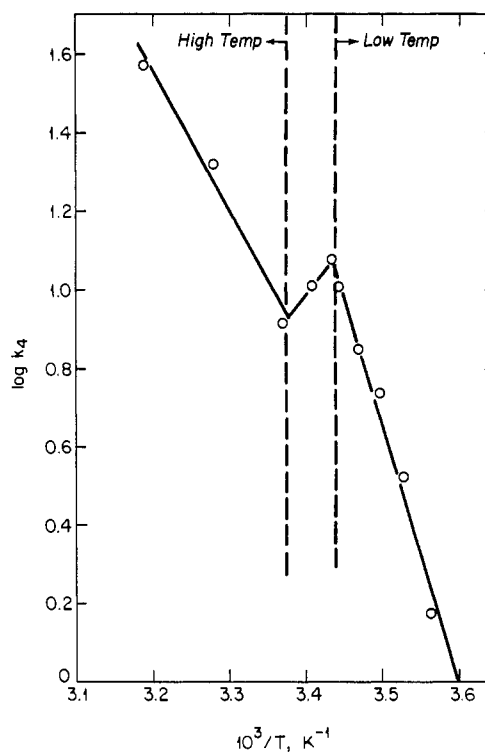


**Figure 9.** Plot of  $\log k_4$  vs  $1/T$  ( $\text{K}^{-1}$ ) for the monotransmetalation of excess  $(\mu_4\text{-O})\text{N}_4\text{Cu}(\text{Ni}(\text{H}_2\text{O}))_3\text{Cl}_6$  (D) with  $\text{Zn}(\text{NS})_2$  ( $\text{B}_3$ ) in nitrobenzene.

data are in Table IV). Second, we can obtain values of  $k_4$  for comparison with the first-order rate constants of rate law 4.<sup>9-11</sup> Third, it turns out that we can demonstrate that there are *two* moderately stable precursor types in a particular transmetalation system governed by rate law 6. This enables direct examination of the relationship between precursor stability and reaction rate.

**Kinetics of Monotransmetalation of  $(\mu_4\text{-O})\text{N}_4\text{Cu}(\text{Ni}(\text{H}_2\text{O}))_3\text{Cl}_6$  (D) by  $\text{Co}(\text{NS})_2$  in Nitrobenzene.** Figures 3 and 5<sup>16</sup> demonstrate that the title reaction is governed by rate law 6. The lowest plot in Figure 3 shows that the title system is governed by rate law 4 at the lowest practical reaction temperature (8.0 °C) in nitrobenzene.

The linear plot of  $\log k_4$  versus  $1/T$  in Figure 7 accommodates kinetic data over the whole temperature range of this study and further demonstrates that rate law 4 is a special case of rate law 6 where  $\beta_1$  is or becomes especially large under particular experimental conditions.<sup>10</sup>

Figure 8 shows a plot of  $\ln \beta_1$  versus  $1/T$ . From this plot we can conclude that the title reaction involves a single precursor with

(21) Wilkins, R. G. *The Study of Kinetics and Mechanism of Reactions of Transition Metal Complexes*; Allyn and Bacon: Boston, MA, 1974.  
 (22) Katakis, D.; Gordon, G. *Mechanisms of Inorganic Reactions*; Wiley-Interscience: New York, 1987.  
 (23) Piskiewicz, D. *Kinetics of Chemical and Enzyme-catalyzed Reactions*; Oxford University Press: New York, 1977.

(24) Al-Shehri, S.; Davies, G.; El-Sayed, A.; El-Toukhy, A. *Inorg. Chem.*, following paper in this issue.

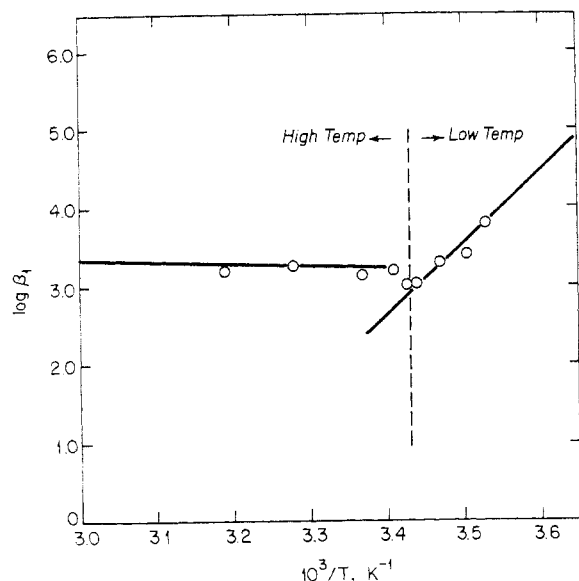


**Figure 10.** Plot of  $\log \beta_1$  vs  $1/T$  ( $K^{-1}$ ) for the reaction of excess  $(\mu_4\text{-O})\text{N}_4\text{Cu}(\text{Ni}(\text{H}_2\text{O}))_3\text{Cl}_6$  (D) with  $\text{Zn}(\text{NS})_2$  ( $\text{B}_3$ ) in nitrobenzene.

$\beta_1 = 3300 \text{ M}^{-1}$  at  $23^\circ\text{C}$ ,  $\Delta H_{\beta_1} = -2.2 \pm 0.3 \text{ kcal mol}^{-1}$ , and  $\Delta S_{\beta_1} = 9 \pm 4 \text{ cal deg}^{-1} \text{ mol}^{-1}$  in nitrobenzene at  $25^\circ\text{C}$ . These data are included in Table IV.

**Kinetics of Monotransmetalation of  $(\mu_4\text{-O})\text{N}_4\text{Cu}(\text{Ni}(\text{H}_2\text{O}))_3\text{Cl}_6$  (D) by  $\text{Zn}(\text{NS})_2$  in Nitrobenzene.** We now come to the most informative system of this study, namely the monotransmetalation of  $(\mu_4\text{-O})\text{N}_4\text{Cu}(\text{Ni}(\text{H}_2\text{O}))_3\text{Cl}_6$  by  $\text{Zn}(\text{NS})_2$  in nitrobenzene. This system contains the most complete detail so far obtained concerning the factors involved in specific, efficient monotransmetalation.

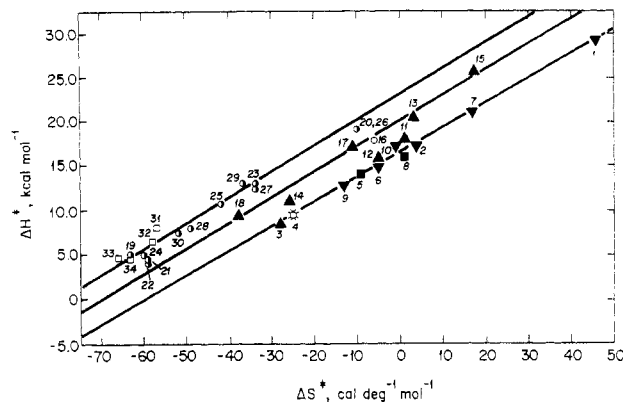
Figures 4 and 6<sup>16</sup> show that rate law 6 governs the title transmetalation system. Figure 9 demonstrates the validity of rate law 6 over two regions of the total experimental temperature range. Note that this kinetic system obeys rate law 4 at the lowest practical temperature (Figure 4), as found in the corresponding  $\text{Co}(\text{NS})_2$  system (Figure 3). However, different reacting systems clearly exist at different temperatures with  $\text{Zn}(\text{NS})_2$  as the transmetalator.

Figure 10 shows a plot of  $\log \beta_1$  versus  $1/T$  for the title system. It is again very evident that there are two regions of different behavior at high and low temperature. In the "high"-temperature region we observe a system that involves a nearly thermoneutral equilibrium 5 ( $n = 1$ ; Table IV), whereas the same system exhibits strongly exothermic character in the "low"-temperature region. We emphasize that a very careful study at closely similar temperatures was made in this system to identify the point of crossover between these two temperature regimes.

The data in Figure 10 are sure proof that there are two major identifiable 1:1 precursor types in transmetalation systems. In this context, "identifiable" means *associated with measured equilibrium parameters*. The thermodynamic parameters for the two precursors involved in the title transmetalation system are included in Table IV.

Figure 9 shows that these two precursors are converted to products in reactions with different activation parameters. We again emphasize that very careful measurements were made of the temperature dependence of this system to identify the crossover region. Figures 9 and 10 indicate the existence of about equal proportions of the two precursors near  $20^\circ\text{C}$ .

Comparison of Figures 8 and 10 shows that changing the transmetalator of  $(\mu_4\text{-O})\text{N}_4\text{Cu}(\text{Ni}(\text{H}_2\text{O}))_3\text{Cl}_6$  from  $\text{Co}(\text{NS})_2$  to  $\text{Zn}(\text{NS})_2$  at low temperature provides access to a type of precursor that is formed much more exothermically. The entropy of formation of this precursor is the most negative of all the equilibrium systems in Table IV. From Figure 9 we see that this precursor would be converted to products at a higher first-order rate than the precursor that actually exists at higher experimental temperatures.



**Figure 11.** Plots of  $\Delta H^*$  ( $\text{kcal mol}^{-1}$ ) vs  $\Delta S^*$  ( $\text{cal deg}^{-1} \text{ mol}^{-1}$ ) for the first-order rate systems. Numbers 1–6 refer to the monotransmetalations of  $(\mu_4\text{-O})\text{N}_4\text{Cu}(\text{Ni}(\text{H}_2\text{O}))_3\text{Cl}_6$  (D) with  $\text{M}(\text{NS})_2$  and  $\text{M}(\text{NS})_3$  in nitrobenzene, where  $\text{M} = \text{Zn}$  ( $\blacktriangledown$ ),  $\text{Co}(\text{II})$  ( $\blacktriangle$ ),  $\text{Co}(\text{III})$  ( $\ast$ ), and  $\text{Cu}(\text{II})$  ( $\blacksquare$ ).<sup>24</sup> Numbers 7 and 8 refer to the reactions of  $(\mu_4\text{-O})\text{N}_4\text{Cu}_2(\text{Ni}(\text{H}_2\text{O}))_3\text{Cl}_6$  with  $\text{M}(\text{NS})_2$ , where  $\text{M} = \text{Zn}$  ( $\blacktriangledown$ )<sup>24</sup> and  $\text{Cu}(\text{II})$  ( $\blacksquare$ ).<sup>24</sup> Numbers 9–12 refer to the monotransmetalations of  $(\mu_4\text{-O})\text{N}_4\text{Cu}_2\text{Br}_6$  with  $\text{M}(\text{NS})_2$ , where  $\text{M} = \text{Zn}$  ( $\blacktriangledown$ ), and  $\text{Co}(\text{II})$  ( $\blacktriangle$ ).<sup>9</sup> Numbers 13–18 refer to the monotransmetalations of  $\text{L}_2\text{Cu}_2\text{X}_2\text{Y}$  with  $\text{M}(\text{NS})_2$ , where  $\text{M} = \text{Co}$  ( $\blacktriangle$ ) and  $\text{Zn}$  ( $\blacktriangledown$ ).<sup>10</sup> Numbers 19–30 refer to the isomerizations of unassociated  $(\mu_2\text{-O})\text{N}_2\text{Cu}_2(\text{Ni}(\text{H}_2\text{O}))_2\text{Cl}_4$  and  $(\mu_2\text{-CO}_3)\text{N}_2\text{Cu}_2(\text{Ni}(\text{H}_2\text{O}))_2\text{Cl}_4$  complexes.<sup>25</sup> Numbers 31–34 refer to the isomerizations of unassociated  $\text{N}_3\text{Cu}_2(\text{Ni}(\text{H}_2\text{O}))_2\text{Cl}_4\text{O}_2$  and  $\text{N}_3\text{Cu}(\text{Ni}(\text{H}_2\text{O}))_3\text{Cl}_4\text{O}_2$  complexes.<sup>26</sup>

#### Activation Parameter Correlation for First-Order Systems.

Figure 11 shows activation parameter correlations for all the first-order systems involving dimeric and tetrameric copper(II) molecules from this and related<sup>9–11,24–26</sup> work. Data from rate laws 4 and 6 are correlated, which indicates that  $k_4$  is the limiting rate constant of rate law 6.

The correlations shown are very striking. All the lines have the same slope ( $300 \pm 25 \text{ K}$ ). The lowest line correlates data for irreversible transmetalation systems, first-order complexation reactions with  $\text{Cu}(\text{NS})_2$ ,<sup>11,24</sup> and activation parameters  $\Delta H_r^*$  and  $\Delta S_r^*$  for the  $k_r$  term of rate law 12. This term governs the dissociation of complexes of the form  $\text{T-Cu}(\text{NS})_2$ .<sup>11,24</sup>

The data for first-order transmetalation reactions of  $\text{L}_2\text{Cu}_2\text{X}_2(\text{CO}_3)$  targets are correlated by the middle line of Figure 11. Since  $\text{L}_2\text{Cu}_2\text{X}_2(\text{CO}_3)$  targets are known to contain terminal halide, then the especially stable precursors of these systems must contain terminal halide.<sup>10</sup> The parallelism of the two lower lines of Figure 11 is a strong indication that all of the first-order dissociation reactions of complexes  $\text{T-Cu}(\text{NS})_2$  that are governed by rate law 12<sup>11,24</sup> involve species containing terminal halide.

The top line of Figure 11 correlates data for the isomerization of  $(\mu_2\text{-Y})\text{N}_2\text{Cu}_2(\text{Ni}(\text{H}_2\text{O}))_2\text{X}_4$ <sup>25</sup> and  $(\mu_4\text{-O}, \mu_2\text{-O})\text{N}_n\text{Cu}_{4-x}(\text{Ni}(\text{H}_2\text{O}))_x\text{X}_4$ <sup>26</sup> complexes. These reactions are all driven by the formation of copper(II) centers containing three-coordinated halide ligands.<sup>25,26</sup> The very negative entropies of activation for these reactions have been interpreted to indicate that the formation of four-membered rings  $\text{Cu} \cdots \text{X} \cdots \text{Ni} \cdots \text{X}$  is required to allow the metal movement that leads to isomerization. The activation process for metal movement requires the breaking of bonds from copper(II) to X, O, and  $\text{CO}_3$  bridging groups, as indicated by an increase in  $\Delta H_{\text{isom}}^*$  as the bridging systems become more extensive.<sup>25</sup>

All the species involved in the correlation of first-order data in Figure 11 contain copper centers that are held in place by bridging halide and, in most cases,<sup>27</sup> oxide or carbonate. The parallelism of all three lines indicates that the breaking of such bridging bonds is a primary requirement for all the processes that are correlated. The main contribution to activation must be the

(25) Cai, G.-Z.; Davies, G.; El-Toukhy, A.; Gilbert, T. R.; Henary, M. *Inorg. Chem.* **1985**, *24*, 1701.

(26) Davies, G.; El-Sayed, M. A.; El-Toukhy, A.; Henary, M.; Martin, C. A. *Inorg. Chem.* **1986**, *25*, 4479.

(27) The exception is the inclusion of data for the dissociation of  $\text{L}_2\text{Cu}_2\text{X}_2\text{M}(\text{NS})_2$  complexes governed by the first-order  $k_r$  term of eq 12.<sup>11</sup>

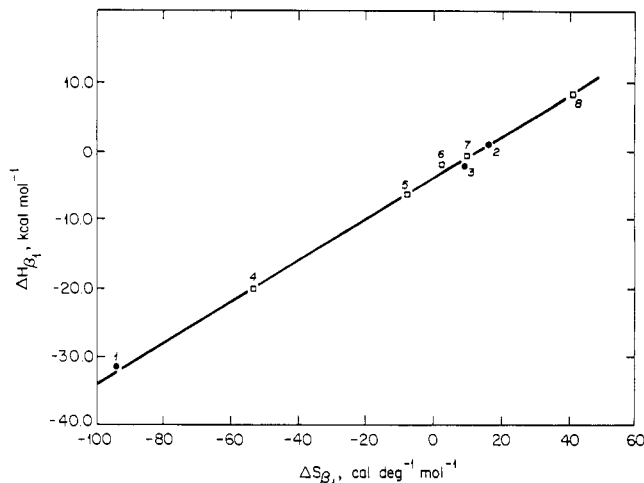


**Figure 12.** Plots of  $\Delta H_{\beta_1}$  (kcal mol<sup>-1</sup>) vs  $\Delta S_{\beta_1}$  (cal deg<sup>-1</sup> mol<sup>-1</sup>) for the following systems:  $(\mu_4\text{-O})\text{N}_4\text{Cu}(\text{Ni}(\text{H}_2\text{O}))_3\text{Cl}_6$  (D) with  $\text{Zn}(\text{NS})_2$  ( $\text{B}_3$ ) in nitrobenzene at low temperature (1);  $(\mu_4\text{-O})\text{Cu}(\text{Ni}(\text{H}_2\text{O}))_3\text{Cl}_6$  (D) with  $\text{Zn}(\text{NS})_2$  ( $\text{B}_3$ ) in nitrobenzene at high temperature (2);  $(\mu_4\text{-O})\text{N}_4\text{Cu}(\text{Ni}(\text{H}_2\text{O}))_3\text{Cl}_6$  (D) with  $\text{Co}(\text{NS})_2$  ( $\text{B}_1$ ) in nitrobenzene (3);  $(\mu_4\text{-O})\text{N}_4\text{Cu}_4\text{Cl}_6$  (A) with  $\text{Cu}(\text{NS})_2$  (NS = *S*-methyl isopropylidenehydrazinecarbodithioate) in nitrobenzene (4);<sup>24</sup>  $(\mu_4\text{-O})\text{N}_4(\text{Ni}(\text{H}_2\text{O}))_3\text{Cl}_6$  with  $\text{Cu}(\text{NS})_2$  (NS = *S*-methyl isopropylidenehydrazinecarbodithioate) in nitrobenzene (5);<sup>24</sup>  $(\text{TEED})_2\text{Cu}_2\text{Cl}_2$  with  $\text{Co}(\text{NS})_2$  ( $\text{B}_1$ ) in nitrobenzene (6);<sup>10</sup>  $(\text{TEED})_2\text{Cu}_2\text{Cl}_2$  with  $\text{Cu}(\text{NS})_2$  (NS = *S*-methyl benzylidenehydrazinecarbodithioate) in nitrobenzene (7);<sup>10</sup>  $(\text{TEED})_2\text{Cu}_2\text{Br}_2$  with  $\text{Cu}(\text{NS})_2$  (NS = *S*-methyl benzylidenehydrazinecarbodithioate) in nitrobenzene (8).<sup>10</sup>

breaking of different Cu–X and Cu–O bonds to account for the appearance of three *separate* lines in Figure 11.

With this interpretation we see that the bridging Cu–X and Cu–O bonds that have to be broken for first-order (a) irreversible transmetalation, (b) complexation,<sup>11,24</sup> (c) adduct dissociation,<sup>11,24</sup> and (d) isomerization<sup>25,26</sup> are weakest for  $(\mu_4\text{-O})\text{N}_4\text{Cu}_{4-x}\text{M}_x\text{X}_6$  complexes (the lowest line in Figure 11) and strongest for  $(\mu_2\text{-Y})_2\text{N}_2\text{Cu}_2(\text{Ni}(\text{H}_2\text{O}))_2\text{X}_4$  and  $(\mu_4\text{-O}, \mu_2\text{-O})\text{N}_n\text{Cu}_{4-x}(\text{Ni}(\text{H}_2\text{O}))_x\text{X}_4$  complexes (as indicated by the uppermost line in Figure 11).

#### Equilibrium Parameters for Precursor and Complex Formation.

Table IV contains equilibrium data for eight precursor and complex formation systems. The equilibrium constants  $\beta_1$  (eq 5) or  $K_1$  (eq 12) range from 250 to 3300 M<sup>-1</sup> at 23 °C. They are much larger than those for formation of adducts  $\text{Ni}(\text{NS})_2\cdot 2\text{py}$  where py is a monodentate pyridine.<sup>12,28</sup> This is mild support for multiple interactions in the precursors and complexes under discussion here. The latter systems range from essentially thermoneutral to strongly exothermic. The entropies of formation range from 41 to –94 cal deg<sup>-1</sup> mol<sup>-1</sup>, with an average of  $-10 \pm 30$  cal deg<sup>-1</sup> mol<sup>-1</sup>. The constant value  $\Delta S_{\beta_1} = -25$  cal deg<sup>-1</sup> mol<sup>-1</sup> from literature data for  $\text{Ni}(\text{NS})_2\cdot\text{py}$  formation<sup>12</sup> was assumed in the previous<sup>9,10</sup> analyses of second-order monotransmetalation rate data. We now see that  $\Delta S_{\beta_1}$  are very reactant-dependent.

**Existence of Two Identifiable Precursor Types in Transmetalation and Complexation Systems.** Figure 12 shows a plot of the enthalpy of formation versus the entropy of formation for all transmetalation and complexation systems that give direct kinetic evidence for association between the reactants from rate law 6 or 12.<sup>11,24</sup> The data come from Table IV. It is evident from this plot that the thermodynamic data for precursor and complex formation are strongly correlated, which suggests the same broad structural features involving the sharing of common atoms by the reactants. The correlation in Figure 12 covers a wide range of target and transmetalator types and stabilities (Table IV). We note in particular that most of the complex-forming systems involve

(28) The largest reported equilibrium constant for formation of  $\text{Ni}(\text{NS})_2\cdot 2\text{py}$  complexes is  $71 \pm 4$  M<sup>-2</sup> in benzene at 25 °C with NS = *S*-methyl *p*-chloroarylidenehydrazinecarbodithioate monoanion and py = 4-methylpyridine.<sup>12</sup>

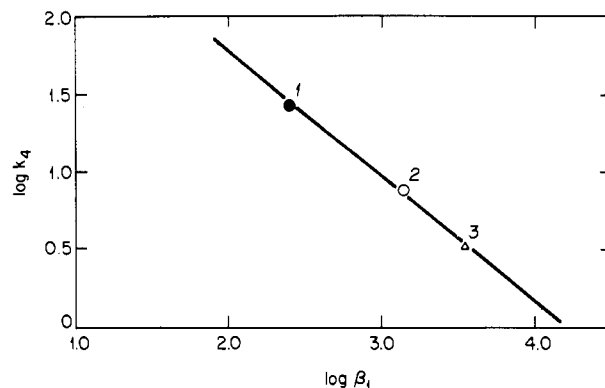


**Figure 13.** Plot of  $\log k_4$  vs  $\log \beta_1$  at 25 °C for the following systems:  $(\mu_4\text{-O})\text{N}_4\text{Cu}(\text{Ni}(\text{H}_2\text{O}))_3\text{Cl}_6$  (D) with  $\text{Zn}(\text{NS})_2$  ( $\text{B}_3$ ) in nitrobenzene at low temperature (1); D with  $\text{Zn}(\text{NS})_2$  ( $\text{B}_3$ ) in nitrobenzene at high temperature (2); D with  $\text{Co}(\text{NS})_2$  ( $\text{B}_1$ ) in nitrobenzene (3).

especially stable<sup>2,14b</sup> reactants B and C (M = Cu). This suggests that exothermic formation of such 1:1 complexes does not involve NS chelate ring opening. Such chelate ring opening is a more likely possibility for thermodynamically weaker<sup>14b</sup> transmetalators  $\text{B}_1$  and  $\text{B}_3$ .

**Relationship between Precursor Stability and the Rate of First-Order Product Formation.** Figure 13 shows a plot of  $\log k_4$  versus  $\log \beta_1$  at 25 °C for the three systems of this study that are governed by rate law 6. It is evident that increasing precursor stability leads to lower reaction rates.

We note the following with regard to this reactivity trend. The rate law for transmetalation of  $(\mu_4\text{-O})\text{N}_4\text{Cu}(\text{Ni}(\text{H}_2\text{O}))_3\text{Cl}_6$  by  $\text{Co}(\text{NS})_3$  is first-order eq 4 over the temperature range 23.0–45.0 °C (Table II).<sup>16</sup> This indicates that  $\text{Co}(\text{NS})_3$  forms a more stable precursor with  $(\mu_4\text{-O})\text{N}_4\text{Cu}(\text{Ni}(\text{H}_2\text{O}))_3\text{Cl}_6$  than does  $\text{Co}(\text{NS})_2$ , which transmetalates D with rate law 6. At the same time we know that  $\text{Co}(\text{NS})_3$  is less thermodynamically stable than  $\text{Co}(\text{NS})_2$ .<sup>14b</sup> Thus, if  $\text{Co}(\text{NS})_2$  forms any kind of ring-opened precursor with  $(\mu_4\text{-O})\text{N}_4\text{Cu}(\text{Ni}(\text{H}_2\text{O}))_3\text{Cl}_6$ , then so should  $\text{Co}(\text{NS})_3$ , and the latter precursor should be the more stable. We find, as expected, that  $k_4$  (23 °C) is 5.5 s<sup>-1</sup> when the transmetalator of D is  $\text{Co}(\text{NS})_2$  and 1.5 s<sup>-1</sup> when it is  $\text{Co}(\text{NS})_3$  (Table III).<sup>30</sup>

**Conclusions.** The transmetalation and complexation of poly-metallic halo amine complexes by  $\text{M}(\text{NS})_n$  reagents involves precursors whose stabilities depend on the reactants. Rate law 6 provides direct access to the relationship between precursor stability and reactivity. We are actively seeking (a) further examples of systems governed by this particular rate law and (b) molecular structures for  $(\mu_4\text{-O})\text{N}_4\text{Cu}_{4-x}\text{M}_x\text{X}_6\cdot\text{Cu}(\text{NS})_2$  complexes. Our findings will be reported in future papers.

**Acknowledgment.** This work was supported by Biomedical Research Support Grant RR07143 from the Department of Health and Human Services and Grants INT-8715384 and CHE8717556 from the National Science Foundation, which are gratefully acknowledged. S.A.-S. thanks the Saudi Arabian Government for a graduate fellowship, and M.A.E.-S. and A.E.-T. thank Alexandria University, Alexandria, Egypt, for study leave to collaborate on this project.

**Supplementary Material Available:** Table II, containing kinetic data for monotransmetalation of D, and Figures 5 and 6, showing plots of eq 11 for the data in Figures 3 and 4 (6 pages). Ordering information is given on any current masthead page.

(29) We have extrapolated the “low-temperature” data for  $k_4$  and  $\beta_1$  in Figures 9 and 10, respectively, over a small range to allow construction of Figure 13 at 25 °C.

(30) Compliance of the D/E monotransmetalation system to rate law 4 would require that  $\beta_1[\text{D}] > 10$  in the denominator of rate law 6 at the lowest [D] employed ( $2.5 \times 10^{-4}$  M; Table II). This gives  $\beta_1 > 4 \times 10^4$  M<sup>-1</sup> at 23 °C, where  $k_4 = 1.5$  s<sup>-1</sup> (Table III). Assuming that the relationship in Figure 13 holds for all monotransmetalations of D with rate law 6, a short extrapolation to  $\log 1.5 = 0.18$  predicts  $\beta_1 = 1.5 \times 10^4$  M<sup>-1</sup> for the D/E system at 23 °C. This estimate is of the right order of magnitude to account for the kinetic properties of the D/E system.